International Journal of Microwave and Wireless Technologies, 2017, 9(2), 357–363.
doi:10.1017/S1759078715001476

RESEARCH PAPER

Novel compact dual-band-notched ultra-wideband printed antenna with a parasitic circular ring strip

ZHIJUN TANG, XIAOFENG WU, ZAIFANG XI AND SHIGANG HU

A simple and compact printed ultra-wideband antenna with dual-band-notched characteristics is presented. The proposed antenna is composed of a rectangular patch and a modified ground plane. The rectangular patch is etched onto a lossy FR4 substrate. A circular ring strip parasitizes the rectangular patch embedded by a U-shaped slot. Two inverted-L slits and a rectangular slit are embedded onto the ground plane. Some bandwidth enhancement and band-notched techniques are applied in the antenna structure for broadening the bandwidth and generating notches. The simulated and measured results show that the proposed antenna offers a very wider bandwidth ranging from 3.04 to 17.30 GHz, defined by the return loss less than −10 dB, with dual-notched bands of 3.30–4.20 and 5.10–5.85 GHz covering the 3.3/3.7 GHz WiMAX, 3.7/4.2 GHz C-band, and 5.2/5.8 GHz wireless local area network systems. Furthermore, the proposed antenna presents relatively high antenna gain and quasi-omnidirectional radiation patterns.

Keywords: Ultra wideband antenna, Dual-notched bands, Parasitic strip, Slot antenna

Received 20 March 2015; Revised 4 September 2015; Accepted 14 September 2015; first published online 9 October 2015

I. INTRODUCTION

As the key component of a wireless communication system, antenna directly determines the quality of service for communication application. In order to cover more wireless communication services, there is an increasing demand for antennas capable of operating at an extremely wider frequency band such as ultra-wideband (UWB) [1–2]. UWB is a high-speed radio technology that is used at very low-power levels for short-range wide bandwidth communication using a large portion of the radio spectrum [3]. According to FCC regulation (2002) and IEEE 802.15.3a standard (2004), ultra-wideband communication frequency band is identified as 3.1–10.6 GHz. Therefore, the feasible design and implementation of UWB systems have become a highly competitive topic in both academic and engineering fields of wireless communication applications [4]. Recently, much attention has been focused on UWB communication systems. These systems are suitable candidates for exchanging high-rate information. To achieve such high-performance communication systems, UWB antennas should be effective in transmitting, compact, non-dispersive, and have a good wide impedance bandwidth properties. These features are desirable for both indoor and outdoor UWB applications. In order to satisfy such requirements, various planar antennas have been developed for UWB communications over the last few years. A large number of patch antennas have been introduced to give better performances for a variety of UWB applications due to the low performance of wire antennas. Due to their simple geometric structures and ease of fabrication, the proposed UWB antennas mainly focus on the slot and monopole antennas. Broadband planar monopole antennas have received considerable attention owing to their attractive merits, such as ultra-wide frequency band, good radiation properties, simple structure, and ease of fabrication. In these literatures, many different microstrip UWB antennas with rectangular, circular, triangular, elliptical, hexagonal, and so on patches are currently being considered for UWB applications [5, 6].

However, the frequency range for UWB systems can cause interferences to the existing WiMAX, C-band, and wireless local area network (WLAN) system operating at 3.30–3.70 GHz, 3.70–4.20, and 5.20 GHz (5.150–5.350 GHz)/5.80 GHz (5.725–5.825 GHz), respectively, which result in overloading with the UWB systems. The conventional UWB antennas are difficult to meet these requirements. In order to avoid interferences among these systems, it is necessary to design UWB antenna with these notched notches. Recently, various band-notched antennas were proposed in the past several years [7–29]. Some techniques have been proposed for achieving band-notched characteristic by embedding various types of slots onto the radiating patch and using a defected ground structure. However, the notched band is usually generated using only single resonator and cannot offer a precise selectivity to meet the requirements in most existing band-notched antennas. Furthermore,

College of Information and Electrical Engineering, Hunan University of Science and Technology, Xiangtan 411201, China. Phone: +86073158290114
Corresponding author:
Z. Tang
Email: zjtang@hnust.edu.cn

bandwidth and gain are important parameters for design a band-notched UWB antenna. Most existing band-notched antennas are only obtained about bandwidth of 3.0–12 GHz or the gain of 2.0 dBi.

In this paper, a novel compact printed antenna is constructed by a rectangular radiating patch, a mirostrip transmission line, a printed circuit board (PCB) substrate, and a defected ground plane. A parasitic circular ring strip and a U-shaped slot with different widths are embedded onto the radiating patch. The proposed antenna can achieve a compact planar profile, wider impedance bandwidth (3.04–17.30 GHz), relatively high gain (is larger than 3.0 dBi), stable radiation pattern characteristics. The proposed antenna is suitable for wireless wideband communication applications.

II. ANTENNA DESIGN

The geometry of the proposed antenna is shown in Fig. 1. The antenna consists of a radiating patch, a microstrip feed line and a defected ground plane. The radiator of the antenna is printed on a lossy FR4 substrate of thickness 1.6 mm, a relative permittivity of $\varepsilon_r = 4.4$ and a loss tangent of tan $\delta =$ 0.018. The width of the feed line is W_f. The defected ground plane is etched on the other side of the substrate. It is shown in Fig. 1(a) that a circular ring strip parasitizes the rectangular patch embedded by a U-shaped slot. The U-shaped slot locates the lower part of the rectangular patch, and the widths of the slot are different. By inserting the U-shaped slot into the rectangular patch, a higher frequency band-stop filter is formed. On the other hand, by directly parasitizing the circular ring strip onto the rectangular patch, a lower frequency band-stop filter is also formed for the UWB antenna. Furthermore, the bandwidth of the proposed antenna can be broadened by integrating the U-shaped slot and the parasitic circular ring strip simultaneously. Therefore, the U-shaped slot can produce approximately a notched band range of 5.0–6.0 GHz by adjusting the size and location of the slot. The parasitic circular ring strip parasitizes on the upper part of the rectangular patch, which can produce approximately a notched band range of 3.0–4.5 GHz by tuning the size of the circular ring strip. The width and length of the microstrip feed transmission line are referred as W_f and L_f, respectively. The microstrip feed transmission line is directly connected with the rectangular radiating patch. It is shown in Fig. 1(b) that the ground plane of the antenna is a rectangular patch embedded with two identical inverted-L slits and one rectangular slit. The defected ground plane is printed onto the opposite side of the PCB substrate under the microstrip transmission line. The defected ground plane with the three slits can further broaden the bandwidth range of 8.0–17.5 GHz and improve the radiation performance. As a result, the geometry of the proposed antenna integrated by the U-shaped slot, the parasitic ring strip, and the defected ground plane with different type slits can offer dual-band-notched and very ultra-wide bandwidth characteristics.

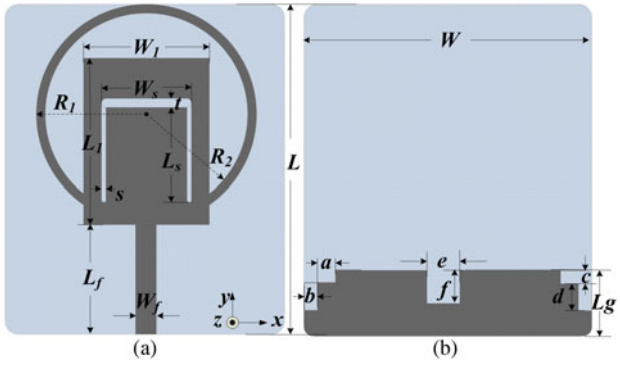

Fig. 1. The antenna physical structure: (a) top view and (b) back view.

III. PARAMETRIC STUDY

The parametric study is carried out to investigate the effects of the antenna parameters on the impedance and a guideline for antenna optimization. It is essential because it provides antenna engineers with more details and characteristics of the antenna. Return loss is an important performance parameter to characterize antenna design. Therefore, the impedance bandwidth of −10 dB return loss (S_{11}) is investigated by simulating and measuring. It has been found that the operating frequency and its band-notched characteristics of the antenna are mainly determined by the size of the U-shaped slot (s, L_s, t), the parasitic circular ring strip (R_1, R_2), microstrip feed line (W_f, L_f), and the defected ground plane (L_g, rectangular slot, inverted-L slot). In the simulated return loss of the antenna, the other parameters are kept to be constant except for these interesting parameters.

Figure 2 shows that the simulated return loss of the proposed antenna varies with different geometrical structure and parameters. It is shown in Fig. 2(a) that the simulated return loss of the antenna varies with changing the sizes of U-shaped slot. The proposed antenna has not a notched band of 5.0–6.0 GHz, if the U-shaped slot is not embedded in the rectangular patch. It shows that the U-shaped slot is a key factor for generating the notched band. Furthermore, the notched band moves from a higher frequency to a lower frequency with the increasing of the parameters s and L_s. In addition, the location of the notched band moves to a higher frequency with the increasing of the parameter t. Figure 2(b) shows that the simulated return loss of the antenna changes with different sizes of the parasitic circular ring strip. As shown in Fig. 2(b), the proposed antenna has not a notched band of 3.0–4.5 GHz if the circular ring strip is not parasitized on the rectangular patch. Moreover, the notched band moves from a lower frequency to a higher frequency with the increasing of the parameters R_1 and R_2. In other words, the circular ring strip is used to generate the notched band for the antenna. Figure 2(c) shows that the simulated return loss of the antenna is influenced by the defected ground plane and its slits. As shown in Fig. 2(c), the impedance bandwidth of the antenna will be narrowed if the rectangular slit or two inverted-L slits are not embedded in the defected ground plane. Figure 2(d) shows that the simulated return loss of the antenna is affected with the size of the microstrip feed line. As shown in Fig. 2(d), the impedance bandwidth of the antenna is sensitive to the width W_f and the length L_f of the feed line. As a result, the impedance bandwidth becomes significantly narrower with either the increasing or the decreasing of W_f and L_f. Therefore, the suitable size of the microstrip feed line is crucial to the antenna design.

https://doi.org/10.1017/S1759078715001476 Published online by Cambridge University Press

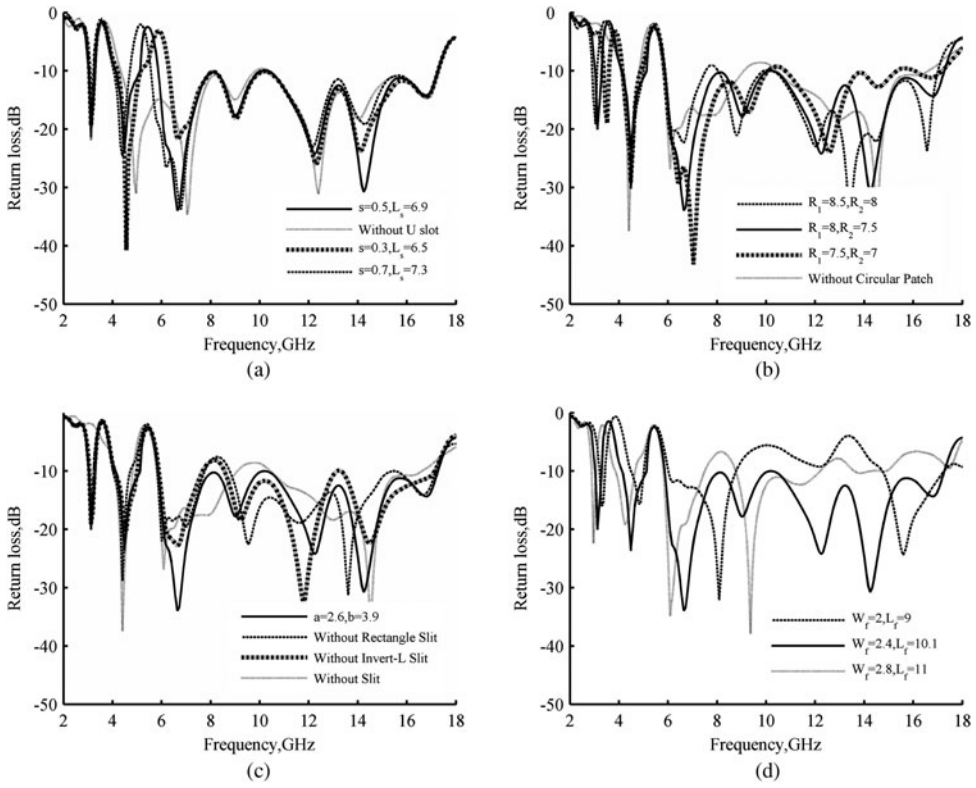

Fig. 2. Simulated return loss of the proposed antenna with different geometrical parameters and structure: (a) the U-shaped slot, (b) the parasitic circular ring, (c) the defected ground plane, and (d) the microstrip feed line.

IV. RESULT AND DISCUSSIONS

According to the above results of parametric study, optimized design parameters of the proposed antenna were found with the following dimensions: $L = 27$ mm, $W = 21$ mm, $L_1 = 12$ mm, $W_1 = 8.5$ mm, $L_f = 10.1$ mm, $W_f = 2.4$ mm, $L_s = 6.1$ mm, $W_s = 6$ mm, $L_g = 8.4$ mm, $R_1 = 8$ mm, $R_2 = 7.5$ mm, $a = 1.5$ mm, $b = 1$ mm, $c = 1.4$ mm, $d = 3$ mm, $e = 2.6$ mm, $f = 3.9$ mm, $s = 0.5$ mm, and $t = 0.8$ mm.

The simulations were carried out using CST Microwave Studio, which is based on the finite-difference time domain and the finite integration technique. To verify the performance of the proposed antenna, reflection and radiation characteristics of the antenna were measured using an Agilent/HP-8720C vector network analyzer.

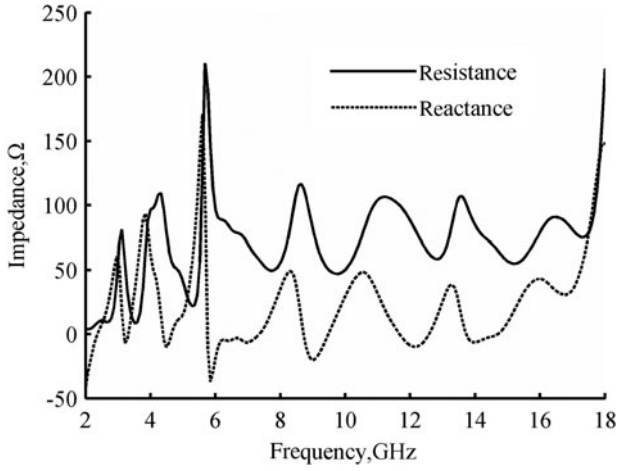

Fig. 3. Simulated impedance of the proposed antenna.

Figure 3 shows the simulated impedance of the antenna. When the operating frequency of the antenna ranges from 2.0 to 18.0 GHz, the proposed antenna's resistances are near to 50 Ω, and the fluctuations of resistance are smaller except for two frequency bands of 3.5–4.5 and 5.0–6.0 GHz. Furthermore, the antenna's reactance fluctuates up and down within the range of zero value except for two separate bands of 3.3–4.2 and 5.0–6.0 GHz. According to the results mentioned above, the proposed antenna has two approximately notched bands of 3.30–4.20 and 5.0–6.0 GHz. Therefore, the proposed antenna can offers an ultra-impedance wideband with dual-band-notched characteristics.

Figure 4 shows simulated current distributions on the radiating patch of the antenna. As shown in Fig. 4(a), it is observed that the current flows are more around the parasitic circular ring strip when the proposed antenna operates at 3.4 GHz. Furthermore, the current flows are oppositely directed between the left and the right parts of the strip. Similarly, it is shown in Fig. 4(b) that the current flows are relatively concentrated on the U-shaped slot edges when the proposed antenna operates at 5.2 GHz, and they are also oppositely directed between the interior and exterior parts of the slot. Therefore, the resultant radiation fields cancel out each other and high attenuations are emerged when the antenna operates at near 3.4 or 5.2 GHz. Furthermore, it shows that the antenna has dual filter structure, which can produce two notched bands.

The fabricated antenna fed by mirostrip line and attached with a SubMiniature version A (SMA) connector is shown in Fig. 5. Figure 6 shows the simulated and measured return loss

https://doi.org/10.1017/S1759078715001476 Published online by Cambridge University Press

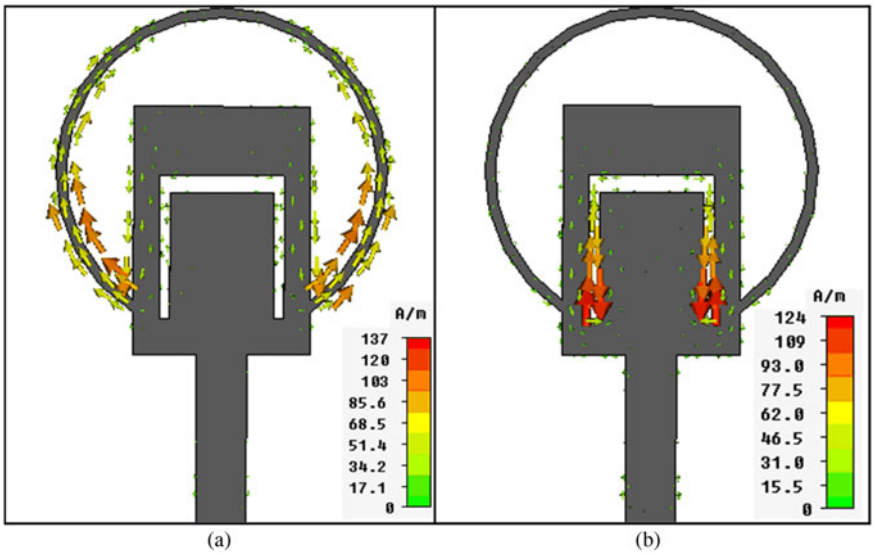

Fig. 4. Simulated current distributions on the radiating patch: (a) 3.4 GHz and (b) 5.2 GHz.

values of the antenna. As shown in Fig. 6, the experimental measurements are basically consistent with the simulated results. The proposed antenna has a very ultra-wide bandwidth of 3.04–17.30 GHz with the dual-notched bands of 3.30–4.2 and 5.10–5.85 GHz. The dual-notched bands are exactly consistent with 3.3/3.7 GHz WiMAX, 3.7/4.2 GHz C-band, and 5.2/5.8 GHz WLAN systems, respectively.

Figure 7 shows the realized gains of the proposed antenna operating at frequency range of 2.0–18.0 GHz. When the proposed antenna operates at frequency range of 3.30–17.30 GHz, it is observed that the minimum realized gain reaches to 3.0 dBi, and the maximum realized gain is 4.8 dBi except for the above-mentioned dual-notched bands. Antenna realized gains become very small when the proposed antenna operates at two notched bands of 3.3–4.2 and 5.10–5.85 GHz. In addition, the realized gain is also affected mainly by the size of the antenna radiating elements and the radiating efficiency. Therefore, the antenna exhibits stable gain characteristics across the three separate operating bands of 3.0–3.3, 4.2–5.1, and 5.85–17.30 GHz.

The *H*-plane radiation patterns of the antenna at four different frequencies of 3, 6, 9, and 12 GHz are shown in Fig. 8, respectively. It is observed that quasi-omnidirectional pattern in the *H*-plane is obtained at the entire band. Furthermore, cross-polarizations of the radiation patterns in *H*-plane are smaller at lower frequencies of 3 and 6 GHz, respectively, while cross-polarizations are larger at 9 and 12 GHz, respectively. As a result, the differences between co-polarizations and cross-polarizations are larger than 20.0 dBi at lower frequencies, and the differences between co-polarizations and cross-polarizations are approximately 10.0 dBi at higher frequencies. It shows that good *H*-plane cross-polarizations are obtained at lower frequencies for the antenna. The *E*-plane radiation patterns of the antenna at frequencies of 3, 6, 9, and 12 GHz are illustrated in Fig. 9, respectively. It is observed that the *E*-plane radiation patterns have two main beams in the broadside direction (-75°, 75°) and (105°, 255°), which exhibit monopole-like patterns in the *E*-plane. Furthermore, it is observed that the *E*-plane radiation patterns at 9 and 12 GHz are not symmetrical compared to the lower

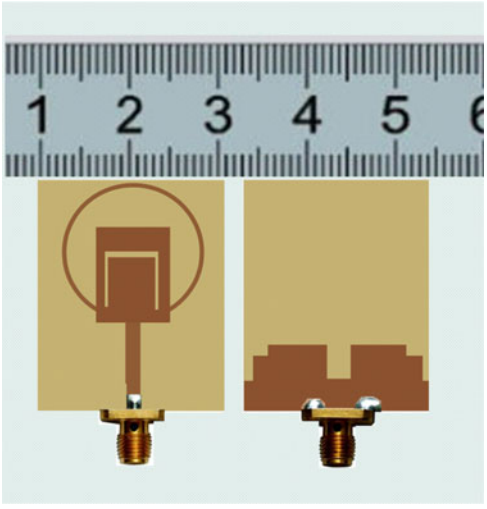

Fig. 5. Fabricated antenna attached with a SMA connector.

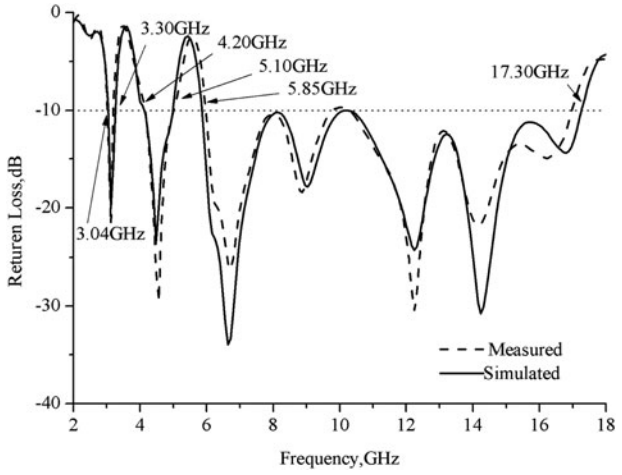

Fig. 6. Measured and simulated return loss of the proposed antenna.

https://doi.org/10.1017/S1759078715001476 Published online by Cambridge University Press

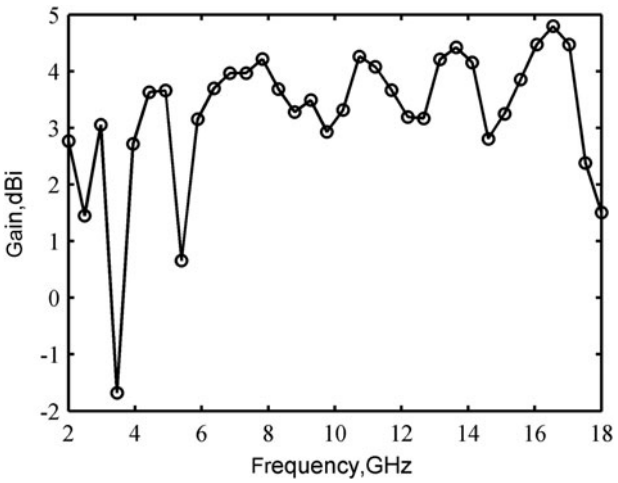

Fig. 7. Realized gain-frequency characteristic curve of the proposed antenna.

frequencies. It is because that the *E*-plane radiation patterns of the antenna are quite similarly to the typical printed monopoles. The *E*-plane radiation patterns are almost symmetrical in the lower bands, while it is directional at the higher bands, which is caused by the antenna structure radiating more electromagnetic waves at higher frequencies. In addition, the *E*-plane cross-polarizations are also small over all operating frequencies. As a result, the differences between co-polarizations and cross-polarizations in *E*-plane are larger than 20.0 dBi, which shows the antenna has good radiation patterns in the *E*-plane.

Group delay refers to a phase difference caused by different signal frequency components transmitting in the same medium because of the existence of the distribution parameters. It is defined as the negative derivative of the phase and angular frequency.

$$\tau = -\frac{d\phi(\omega)}{d\omega}, \tag{1}$$

where τ is group delay, $\phi(\omega)$ is the phase, and ω is the angular frequency. Group delay represents the degree of distortion of pulse signal, which is an important performance parameter for UWB antenna design. As shown in Fig. 10, it can be observed that the variation of group delay is less than 1.0 ns at all operating frequencies of 3.04–17.30 GHz except for two notched bands. Therefore, the proposed antenna has very lower group delay. Especially at around 3.30 and 5.10 GHz, the larger fluctuations of group delay are also observed. The larger fluctuations are caused by the two band-stop filters mentioned above. Furthermore, the group delays are negative delays caused by forward distortion of the phase at around 3.30 GHz, while group delays are positive delays caused by backward distortion of the phase at around 5.10 GHz.

The antenna efficiency is also an important parameter for all antenna design besides UWB antenna, which is equal to the radiation efficiency minus the return loss [7]. The efficiency of the antenna has a minimum value of 84.2% and a maximum value of 94.1% within the frequency range from 3.04 to 17.30 GHz. The average efficiency of the antenna is approximately 92.3%.

VI. CONCLUSION

In this paper, a novel compact UWB planar antenna with dual-notched bands has been proposed and discussed. The

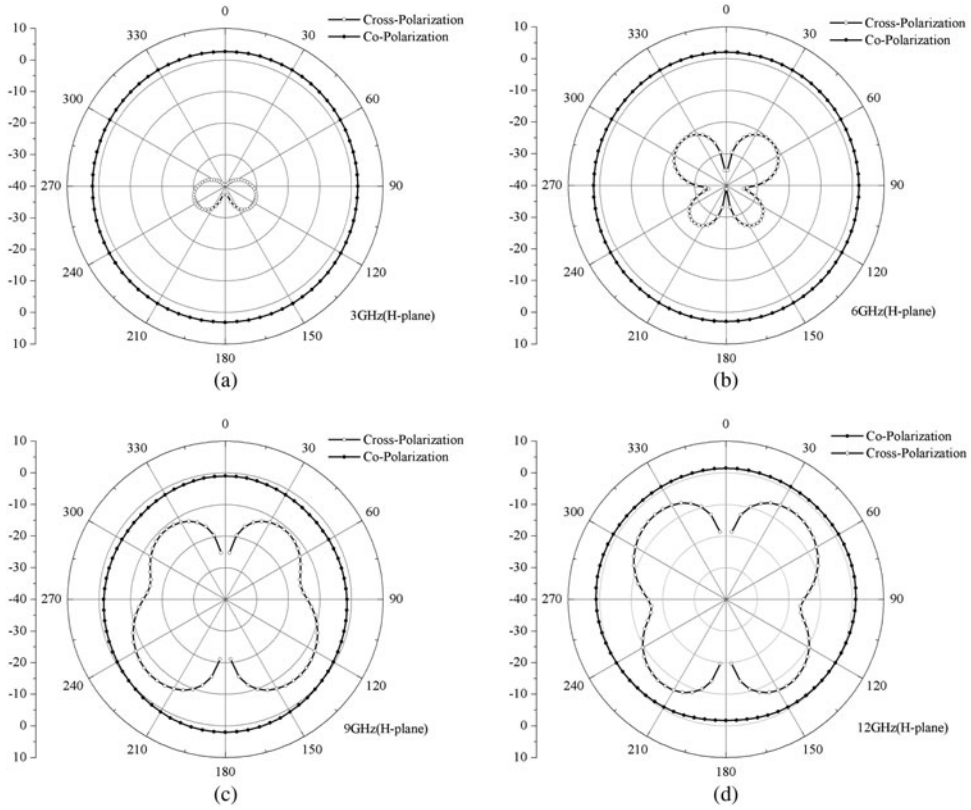

Fig. 8. *H*-plane radiation patterns of the proposed antenna: (a)3 GHz, (b)6 GHz, (c)9 GHz, and (d)12 GHz.

https://doi.org/10.1017/S1759078715001476 Published online by Cambridge University Press

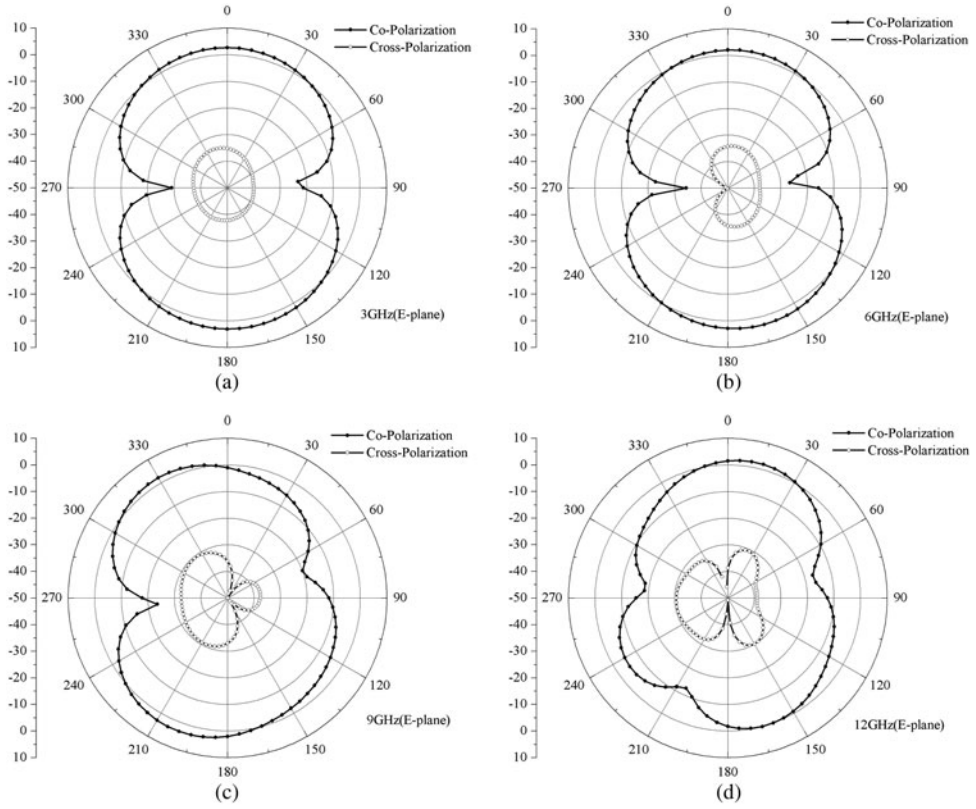

Fig. 9. *E*-plane radiation patterns of the proposed antenna: (a)3 GHz, (b)6 GHz, (c)9 GHz, and (d)12 GHz.

characteristics of the proposed antenna have been investigated numerically and justified experimentally. Dual notched bands are realized using a U-shaped slot and a parasitic circular ring strip in a rectangular radiating patch. Furthermore, the bandwidth of the proposed antenna can be further broadened by embedding a rectangular slit and two identical inverted-L slots in a defected ground plane. As a result, the proposed antenna presents not only dual-notched bands of 3.30–4.20 and 5.10–5.85 GHz, but also a very wide bandwidth range from 3.04 to17.30 GHz. In addition, the proposed antenna has a relatively high gain at all operating frequencies except for the dual-notched bands. Especially, the proposed antenna has nearly omnidirectional radiation patterns in the *H*-plane and monopole-like radiation patterns in the *E*-plane. Therefore, the proposed antenna can meet the requirements of wireless UWB communication applications.

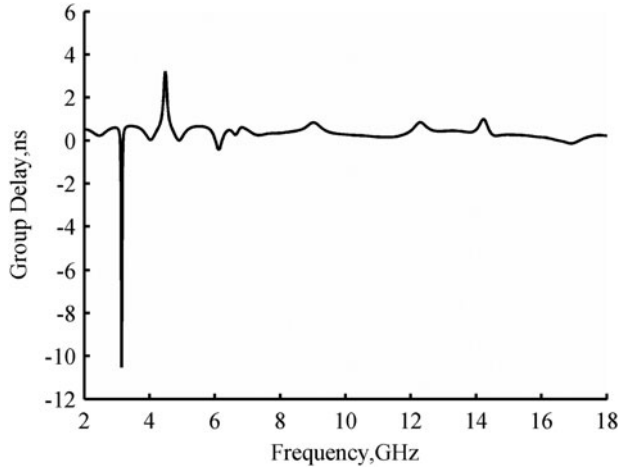

Fig. 10. Group delay time of the proposed antenna.

ACKNOWLEDGEMENTS

This work was supported by the National Natural Science Foundation of China (Grant Nos 61377024, 61274026, and 61376076), the Scientific Research Fund of Hunan Provincial Education Department, China (Grant No. 14B060), and the Science and Technology Plan Project of Hunan Province, China (Grant Nos 2014FJ2017 and 2013FJ2011).

REFERENCES

[1] Tang, Z.J.; Wu, X.F.; Zhan, J.: Novel compact band-notched UWB antenna using convex – shaped slot patch. Microw. Opt. Technol. Lett., **57** (1) (2015), 201–203.

[2] Rezaul, A.; Mohammad, T.I.: Printed planar antenna for wideband applications. Journal of Infrared Millim. Terahertz Waves, **31** (8) (2010), 969–978.

[3] Huang, C.Y.; Su, J.Y.: A printed band-notched UWB antenna using quasi-self- complementary structure. IEEE Antennas Wireless Propag. Lett., **10** (10) (2011), 1151–1153.

[4] Qing, X.; Chen, Z.N.: Compact coplanar waveguide-fed ultra-wideband monopole-like slot antenna. IET Microw. Antennas Propag., **3** (5) (2009), 889–898.

https://doi.org/10.1017/S1759078715001476 Published online by Cambridge University Press

[5] 'Design and characterization of microstrip UWB antennas', http://www.cdn.intechopen.com, accessed 10 January 2015.

[6] Tang, Z.J.; Zhan, J.; Liu, H.L.: Compact CPW-fed antenna with two asymmetric U-shaped strips for UWB communications. Electron. Lett., **48** (14) (2012), 810–812.

[7] Abdollahvand, M.; Dadashzadeh, G.; Mostafa, D.: Compact dual band-notched printed monopole antenna for UWB application. IEEE Antennas Wireless Propag. Lett., **9** (11) (2010), 1148–1151.

[8] Ellis, M.S. et al.: A novel miniature band-notched wing-shaped monopole ultrawideband antenna. IEEE Antennas Wireless Propag. Lett., **12** (12) (2013), 1614–1617.

[9] Jiang, D. et al.: Compact dual-band-notched UWB planar monopole antenna with modified CSRR. Electron. Lett., **48** (20) (2012), 950–951.

[10] Wang, Y.F. et al.: Band-notched UWB rectangular dielectric resonator antenna. Electron. Lett., **50** (7) (2014), 483–484.

[11] Zhang, K.; Li, Y.X.; Long, Y.L.: Band-notched UWB printed monopole antenna with a novel segmented circular patch. IEEE Antennas Wireless Propag. Lett., **9** (12) (2010), 1209–1212.

[12] Lin, C.C.; Jin, P.; Ziolkowski, R.W.: Single, dual and tri-band-notched ultra-wideband (UWB) antennas using capacitively loaded loop (CLL) Resonators. IEEE Trans. Antennas Propag., **60** (1) (2012), 102–108.

[13] Raha, E.; Javad, N.; Changiz, G.: Electromagnetically coupled band-notched elliptical monopole antenna for UWB applications. IEEE Trans. Antennas Propag., **58** (4) (2010), 1397–1402.

[14] Azim, R.; Mobashsher, A.T.; Islam, M.T.: UWB antenna with notched band at 5.5 GHz. Electron. Lett., **49** (15) (2013), 922–924.

[15] Dimitris, E.A. et al.: Reconfigurable UWB antenna with RF-MEMS for on-demand WLAN rejection. IEEE Trans. Antennas Propag., **62** (2) (2014), 602–608.

[16] Li, W.T. et al.: Planar antenna for 3G/bluetooth/WiMAX and UWB applications with dual band-notched characteristics. IEEE Antennas Wireless Propag. Lett., **11** (1) (2012), 61–64.

[17] Ahmad, A.G.; Dimitris, E.A.: Dual band-reject UWB antenna with sharp rejection of narrow and closely-spaced bands. IEEE Trans. Antennas Propag., **60** (4) (2012), 2071–2076.

[18] Nguyen, D.T.; Lee, D.H.; Park, H.C.: Very compact printed triple band-notched UWB antenna with quarter-wavelength slots. IEEE Antennas Wireless Propag. Lett., **11** (4) (2012), 411–413.

[19] Rezaul, A.; Mohammad, T.I.; Ahmed, T.M.: Dual band-notch UWB antenna with single tri-arm resonator. IEEE Antennas Wireless Propag. Lett., **13** (3) (2014), 670–673.

[20] Li, T. et al.: Compact UWB band-notched antenna design using interdigital capacitance loading loop resonator. IEEE Antennas Wireless Propag. Lett., **1** (6) (2012), 724–727.

[21] James, R.K.; Peter, S.H.; Peter, G.: Band-notched UWB antenna incorporating a microstrip open-loop resonator. IEEE Trans. Antennas Propag., **59** (8) (2011), 3045–3048.

[22] Debdeep, S.; Kumar, V.S.; Kushmanda, S.: A compact microstrip-fed triple band-notched UWB monopole antenna. IEEE Antennas Wireless Propag. Lett., **13** (2) (2014), 396–399.

[23] Chu, Q.X.; Mao, C.X.; Zhu, H.: A compact notched band UWB slot antenna with sharp selectivity and controllable bandwidth. IEEE Trans. Antennas Propag., **61** (8) (2013), 3961–3966.

[24] Chuang, C.T.; Lin, T.J.; Chung, S.J.: A band-notched UWB monopole antenna with high notch-band-edge selectivity. IEEE Trans. Antennas Propag., **60** (10) (2012), 4492–4498.

[25] Mohammadian, N.; Azarmanesh, M.N.; Soltani, S.: Compact ultra-wideband slot antenna fed by coplanar waveguide and microstrip line with triple-band-notched frequency function. IET Microw. Antennas Propag., **4** (11) (2010), 1811–1817.

[26] Mohammad, R.G.; Farzad, M.: A compact hexagonal wide-slot antenna with microstrip- fed monopole for UWB application. IEEE Antennas Wireless Propag. Lett., **10** (6) (2011), 682–685.

[27] Tu, Z.h.; Li, W.A.; Chu, Q.X.: Single-layer differential CPW-fed notch-band tapered-slot UWB antenna. IEEE Antennas Wireless Propag. Lett., **13** (7) (2014), 1296–1299.

[28] Valizade, A. et al.: A novel design of reconfigurable slot antenna with switchable band notch and multiresonance functions for UWB applications. IEEE Antennas Wireless Propag. Lett., **11** (10) (2012), 1166–1169.

[29] Nasser, O.; Mohammad, O.; Noradin, G.: Dual band-notched small monopole antenna with novel W-shaped conductor backed-plane and novel T-shaped slot for UWB applications. IET Microw. Antennas Propag., **7** (1) (2013), 8–14.

Zhijun Tang received a bachelor degree in Electrical Engineering from Hunan University in 1998 and received his Ph.D. degree in Electrical Engineering from Hunan University in 2010. Presently he is working as an associate Professor and Director of the Department of Communication Engineering in Hunan University of Science and Technology. He has authored more than 20 research papers and his main research interests are UWB antenna design, RFID electromagnetic modeling, and RFID antenna design.

Xiaofeng Wu received a bachelor degree in Automation from Hunan University of Science and Technology in 1998 and received his Ph.D. degree in Microelectronics from Xidian University in 2010. At present he is the Vice President of School of Information Science and Engineering. His main research interests are design and optimization of high-power microwave power amplifiers.

Zaifang Xi received his Master's degree from the Hunan University in 2003. He became a full Associate Professor at Hunan University of Science and Technology in 2009. His current research interests include signal processing and communication system.

Shigang Hu received his Ph.D. degree in Microelectronics from Xidian University in 2009. He has been working at Hunan University of Science and Technology since 2010. He has authored more than 30 research articles and his current research interests include analog IC design and semiconductor devices.

https://doi.org/10.1017/S1759078715001476 Published online by Cambridge University Press